Vibrational Line Shifts in Supercritical Fluids

S. A. Egorov[†] and J. L. Skinner*

Theoretical Chemistry Institute and Department of Chemistry, University of Wisconsin, Madison, Wisconsin 53706

Received: August 20, 1999; In Final Form: November 24, 1999

A microscopic statistical mechanical theory of solvent-induced vibrational line shifts of dilute solutes in supercritical fluids is presented. The theory is based on a simple model of a spherical solute present at infinite dilution in a fluid of spherical solvent particles. A microscopic expression for the vibrational line shift is given, which involves the solute−solvent radial distribution function and interaction potentials. The distribution function is obtained from integral equations and from Monte Carlo simulations. The theory is applied to study the experimentally observed anomalous density dependence of line shifts in supercritical fluids in the vicinity of the critical point. Model calculations of spectral shifts are performed for a range of solvent densities and temperatures and model potential parameters. In addition, a quantitative comparison of the theory with experimental data on vibrational spectral shifts is performed, and the agreement is satisfactory.

I. Introduction

Supercritical fluids (SCFs) are currently receiving much attention as a result of their unique physical properties.[1−5] The combination of unusually high dissolving power and fast mass-transfer rates makes SCFs attractive alternatives to liquid solvents for a variety of industrial applications, such as extraction, separation, and reaction processes.[2,6,7] In addition, the high compressibility of SCFs in the near-critical region allows one to tune their properties to desired values by applying small changes in pressure, which in turn makes it possible to tailor the rates and selectivities of chemical processes. Since the aforementioned applications of SCFs generally involve dilute solutions, it is essential to develop a microscopic understanding of the structure and dynamics of a supercritical solvent in the vicinity of a single solute molecule. There exists a wealth of experimental data on supercritical solvation involving thermodynamic, transport, and spectroscopic measurements.[1,2] In this work we focus on some spectroscopic studies.

The simplest spectroscopic observable is the steady-state absorption line shape. When a solute is in a solvent, the frequency of the solute's absorption maximum is different from its value for the isolated solute, and the change in frequency is called the solvatochromic shift. Both electronic[8−18] and vibrational[19−26] shifts have been measured for a variety of solute/solvent combinations as a function of solvent density and temperature, and certain characteristic patterns have emerged. In particular, when the line shift is measured as a function of density along an isotherm just above the critical temperature T_c (typically at $T_r \equiv T/T_c \simeq 1.01$), one often observes an initial steep linear density dependence in the low-density regime, followed by a weaker density dependence in the neighborhood of the critical density. In some cases in the near-critical region the line shift is nearly density independent, resulting in a "density plateau". In contrast, when measurements are performed at somewhat higher temperatures (around $T_r \simeq 1.06$ or higher), the frequency shifts display a more nearly linear density dependence throughout the whole density range. It should also be noted that line shift studies on neat fluids seem in general[21,22] (although not always[25]) to show a nearly linear density dependence, even in the near-critical region.

The microscopic origin of the nonlinear density dependence of solvatochromic shifts has been discussed qualitatively in terms of "clustering" or "local density enhancement" of a near-critical solvent around the solute.[4,13,27−42] This interpretation is based on the concept of an "attractive mixture", where the solvent is attracted more strongly to the solute than to itself. As a result, the local environment around a dilute solute can differ dramatically from that around a solvent molecule. Many of the theoretical studies of local density enhancements in attractive mixtures were based on Percus−Yevick (PY) or hybrid mean spherical approximation (HMSA) integral equation results. We have recently shown,[43] from a comprehensive comparison between integral equation and Monte Carlo simulation results, that for attractive mixtures these integral equation closures can lead to very significant errors in the near-critical region. Nonetheless, we believe that the qualitative conclusions drawn from these studies are basically correct.

Theoretical approaches to understanding spectral line shifts in SCFs have been based largely on dielectric continuum theories of solvation.[8,13,33,44] On the other hand, Schwarzer et al.,[10] Adams,[45] and Frankland and Maroncelli[46] have calculated spectral shifts in SCFs from Monte Carlo or molecular dynamics simulations, but have not considered temperatures below $T_r \simeq 1.06$. Ben-Amotz and co-workers have developed a "perturbed hard sphere fluid" microscopic theory,[22,47] which is motivated by the work of Schweizer and Chandler,[48] and have used the theory to analyze data in the near-critical region.[22] Cherayil and Fayer[49] ascribe the origin of the density plateau to scaling aspects of critical phenomena. This approach does not rely on the notion of attractive mixtures, and thereby predicts a density plateau even for cases when the solute is very similar to the solvent, or indeed, for neat fluids.

In this paper we focus on the case of vibrational line shifts, especially in the near-critical regime, and are particularly interested in understanding quantitatively from a molecular

[†] Present address: Department of Chemistry, University of Virginia, Charlottesville, VA 22901.

10.1021/jp992961+ CCC: $19.00
Published on Web 12/31/1999

theory why it is that (1) for a dilute attractive mixture near the critical temperature the line shift shows a nonlinear density dependence, (2) when the temperature is increased the density dependence becomes more linear, and (3) for a neat fluid the density dependence of the line shift is generally nearly linear for near-critical and higher temperatures. Since these three features appear to be more or less universal, it would seem appropriate to study them with simple generic microscopic models. In this spirit, electronic spectra of chromophores in liquids and SCFs have recently been studied with a simple model of a spherical solute present at infinite dilution in a solvent of spherical particles, with all of the molecules interacting through isotropic pairwise potentials.[50−52] As input, the theory requires interaction potentials and radial distribution function. Once the former are specified, the latter can be obtained from the integral equation formalism or from computer simulation.

One possibly problematic issue with implementing the above approach[50,51] in the near-critical region stems from the fact that none of the currently available integral equation theories are capable of producing a correct value for the correlation length exponent (or any of the other exponents for that matter),[53] and as a consequence, the long-range decay of the radial distribution function is not properly described. Even worse, as discussed earlier, for attractive mixtures integral equation results for the short-range aspects of the radial distribution function can be qualitatively in error.[43] Computer simulation results also cannot provide one with scaling properties of near-critical fluids. However, as will be shown, the expression for the solvatochromic shift involves an integral of the solute−solvent radial distribution function times a function related to the solute−solvent interaction potential. Therefore, for short-range interactions (such as Lennard-Jones) the results are insensitive to the behavior of the radial distribution function at long distances. It follows then, that as long as the integral equation theory or computer simulation gives accurate short-range solute−solvent structure, this approach should work well.

The organization of this paper is as follows. In section II we extend the theory presented earlier[50,51] for electronic line shifts to the case of vibrational spectral shifts. In section III we describe our model potentials and the methods we use to calculate the radial distribution functions. In section IV we then perform model calculations of solvatochromic shifts as a function of solvent density at various temperatures and for several sets of model potential parameters. In section V we compare our theoretical results with experimental data[19,22] on vibrational solvatochromic shifts. In section VI we conclude.

II. Microscopic Expression for the Vibrational Line Shift

Our simple generic model involves a single solute with several internal vibrational degrees of freedom immersed in a fluid of spherical solvent particles without internal vibrations. We will assume that the solute interacts with the solvent particles through a spherically symmetric pair potential, $\phi(r, q, \vec{Q})$, which as indicated depends not only on the solute−solvent distance, r, but also on the particular vibrational coordinate of interest, q, and the solute's other vibrational coordinates, $\vec{Q}$. The Hamiltonian is

$$H = H_q + H_{\vec{Q}} + T + \sum_i \phi(r_i, q, \vec{Q}) + \sum_{i<j} \phi_s(r_{ij}). \quad (1)$$

H_q and $H_{\vec{Q}}$ are the (assumed to be uncoupled) vibrational Hamiltonians for mode q and modes $\vec{Q}$, respectively, T is the translational kinetic energy of all particles, r_i is the distance between the ith solvent particle and the solute, $\phi_s(r)$ is the solvent−solvent pair potential, r_{ij} is the distance between solvent particles i and j, and the summation indices run over all solvent particle labels. We will leave the forms of H_q and $H_{\vec{Q}}$ unspecified, simply noting that each has a set of eigenstates and eigenvalues, with quantum numbers n and $\vec{N}$, respectively:

$$H_q|n\rangle = E_n|n\rangle, \quad (2)$$

$$H_{\vec{Q}}|\vec{N}\rangle = E_{\vec{N}}|\vec{N}\rangle. \quad (3)$$

Without loss of generality we can define the solute's internal coordinates so that $q = \vec{Q} = 0$ corresponds to the minimum in the intramolecular potential. We can then define the reference potential $\phi(r) = \phi(r, 0, 0)$, and the perturbation potential

$$\delta\phi(r, q, \vec{Q}) = \phi(r, q, \vec{Q}) - \phi(r). \quad (4)$$

With these definitions we can write the Hamiltonian as

$$H = H_q + H_b + V, \quad (5)$$

where the "system" Hamiltonian H_q is defined as above, the "bath" Hamiltonian H_b involves the translational degrees of freedom and the solute's vibrational modes $\vec{Q}$ and is defined by

$$H_b = H_{\vec{Q}} + T + \sum_i \phi(r_i) + \sum_{i<j} \phi_s(r_{ij}), \quad (6)$$

and V is the system-bath coupling, defined by

$$V = \sum_i \delta\phi(r_i, q, \vec{Q}). \quad (7)$$

Suppose, for example, that one is interested in the vibrational transition from the ground ($n = 0$) state to the first excited ($n = 1$) state for mode q. The zeroth-order frequency for this transition is $(E_1 - E_0)/\hbar$. To first order in perturbation theory, the average frequency shift from this value, $\Delta\omega$, is given by

$$\hbar\Delta\omega = \langle\langle 1|V|1\rangle - \langle 0|V|0\rangle\rangle, \quad (8)$$

where the brackets correspond to an equilibrium average over the bath.

To proceed further, but still keeping the discussion fairly general at this point, we will assume that the solute−solvent potential has the form

$$\phi(r, q, \vec{Q}) = \sum_\alpha A_\alpha(q, \vec{Q}) f_\alpha(r). \quad (9)$$

In other words, it can be written as a sum of terms, each of which is a product of a function of the solute's vibrational coordinates and a function of the solute−solvent distance. In this case the perturbation V can be written as

$$V = \sum_\alpha A_\alpha(q, \vec{Q}) F_\alpha - \sum_i \phi(r_i), \quad (10)$$

where $F_\alpha \equiv \sum_i f_\alpha(r_i)$.

In performing the equilibrium average over the bath we will treat the solute's vibrational modes quantum mechanically, but the translational degrees of freedom classically. Substituting eq 10 into eq 8 then gives

$$\hbar\Delta\omega = \sum_\alpha \lambda_\alpha \langle F_\alpha\rangle \quad (11)$$

where λ_α are temperature-dependent coupling "constants"

determined by details of the solute−solvent interaction potential and the solute's vibrational Hamiltonian, and are given explicitly by

$$\lambda_\alpha = \sum_{\vec{N}} e^{-E_{\vec{N}}/kT}[\langle 1\vec{N}|A_\alpha(q,\vec{Q})|1\vec{N}\rangle - \langle 0\vec{N}|A_\alpha(q,\vec{Q})|0\vec{N}\rangle]/\sum_{\vec{N}} e^{-E_{\vec{N}}/kT}. \quad (12)$$

The classical average of F_α over the translational degrees of freedom can be shown from elementary classical statistical mechanics to be

$$\langle F_\alpha\rangle = \rho\int d\vec{r}\, g(r) f_\alpha(r), \quad (13)$$

where ρ is the solvent number density and $g(r)$ is the solute−solvent radial distribution function appropriate for the translational Hamiltonian

$$H_T = T + \sum_i \phi(r_i) + \sum_{i<j} \phi_s(r_{ij}). \quad (14)$$

Since $f_\alpha(r)$ are typically very short-ranged, the above relation shows, as discussed in the Introduction, that the spectral shift, reflects only the local structure of the solvent around the solute.

III. Model Potentials and the Radial Distribution Function

To perform explicit calculations for solvent-induced spectral shifts, we need to specify solute−solvent and solvent−solvent pair potentials. Given that the potentials are isotropic, and hence we do not consider polar molecules herein, it is natural to assume that the solvent molecules interact with each other with the familiar Lennard-Jones (LJ) form:

$$\phi_s(r) = 4\epsilon_s\left[\left(\frac{\sigma_s}{r}\right)^{12} - \left(\frac{\sigma_s}{r}\right)^{6}\right], \quad (15)$$

where ϵ_s is the well depth and σ_s is the effective diameter of the solvent molecule.

For the pairwise solute−solvent interaction, $\phi(r, q, \vec{Q})$, a potential of the LJ form is also convenient, but in this case the well depth[51,54] and/or the solute−solvent diameter[55] should depend on the solute's vibrational coordinates. So in general we write

$$\phi(r,q,\vec{Q}) = 4\epsilon(q,\vec{Q})\left[\left(\frac{\sigma(q,\vec{Q})}{r}\right)^{12} - \left(\frac{\sigma(q,\vec{Q})}{r}\right)^{6}\right]. \quad (16)$$

Setting $q = \vec{Q} = 0$ defines the reference solute−solvent potential, which in this case also takes the LJ form:

$$\phi(r) = 4\epsilon\left[\left(\frac{\sigma}{r}\right)^{12} - \left(\frac{\sigma}{r}\right)^{6}\right], \quad (17)$$

where of course the well depth and diameter for the reference potential are given by $\epsilon \equiv \epsilon(0,0)$ and $\sigma \equiv \sigma(0,0)$.

To proceed we next expand $\sigma(q, \vec{Q})$ to first order in the vibrational coordinates:

$$\sigma(q,\vec{Q}) \simeq (1 + \gamma q + \sum_j \gamma_j Q_j), \quad (18)$$

where Q_j are the components of $\vec{Q}$. Substituting this into the solute−solvent potential and keeping terms to first order in γ and γ_j gives the potential in the form of eq 9, where

$$A_1(q,\vec{Q}) = 4\epsilon(q,\vec{Q}), \quad (19)$$

$$A_2(q,\vec{Q}) = 24\epsilon(q,\vec{Q})[\gamma q + \sum_j \gamma_j Q_j], \quad (20)$$

$$f_1(r) = \left(\frac{\sigma}{r}\right)^{12} - \left(\frac{\sigma}{r}\right)^{6}, \quad (21)$$

$$f_2(r) = 2\left(\frac{\sigma}{r}\right)^{12} - \left(\frac{\sigma}{r}\right)^{6}. \quad (22)$$

To summarize, then, the frequency shift is obtained from eq 11, together with eqs 12, 13, and the above explicit results for A_1, A_2, f_1, and f_2. λ_1 and λ_2 depend on the differences of certain diagonal matrix elements of A_1 and A_2. Since H_q is in general anharmonic, if A_1 and A_2 are expanded in powers of q, the linear terms will provide the first nonvanishing contributions. Thus we expect the relative magnitude of λ_1 and λ_2 to depend primarily on the relative strength of the dependence on q of $\epsilon(q, \vec{Q})$ and $\sigma(q, \vec{Q})$, respectively. The solute−solvent radial distribution function that appears in eq 13 is for an infinitely dilute LJ mixture where the solvent−solvent well depth and diameter are given by ϵ_s and σ_s, and the solute−solvent well depth and diameter by ϵ and σ. In what follows we will calculate $g(r)$ using the HMSA[56,57] and PY closures to the Ornstein−Zernike integral equation,[58] and from Monte Carlo simulations of up to 2000 particles (we increased the number of particles until converged results were obtained).

IV. Model Calculations for the Line Shift

To present the results of our model calculations, we define the dimensionless density and temperature as $\rho^* = \rho\sigma_s^3$ and $T^* = kT/\epsilon_s$, and the dimensionless distance is defined by $r^* = r/\sigma_s$. The phase diagram of the LJ fluid is known reasonably well from simulation, although the exact location of the critical point is still controversial.[59−61] We will use the values that come from Monte Carlo simulations in the grand canonical ensemble together with a finite-size scaling analysis: $\rho_c^* = 0.316$ and $T_c^* = 1.312$.[59]

We have performed model calculations for the following two sets of solute−solvent pair potential parameters: $\epsilon = \epsilon_s$, $\sigma = \sigma_s$, $\lambda_2 = 0$; and $\epsilon = 2.47\epsilon_s$, $\sigma = 1.22\sigma_s$, $\lambda_2 = 0$. The first set corresponds to a neat LJ fluid, while the second set is an attractive mixture roughly corresponding to Xe in Ne.[43,57] For these calculations we are considering the case where the primary dependence of the solute−solvent potential on q comes from the well depth, and so in both cases $\lambda_2 = 0$. (At the end of this section we will briefly discuss the case where $\lambda_2 \neq 0$.)

For each set of potential parameters we have calculated line shifts for the isotherms at $T^* = 1.338$, 1.41, and 1.70, corresponding respectively to reduced temperatures ($T_r = T/T_c$) of 1.02, 1.07, and 1.30. Our results for $\omega^* \equiv \hbar\Delta\omega/\lambda_1$ from eq 11 for the neat fluid are shown in Figure 1. First of all, one sees that at all temperatures the simulation, HMSA, and PY results are all in good agreement (although for the lowest temperature we could not obtain converged HMSA results near the critical density). Second, note that although the results are not precisely linear in density at all three temperatures, they are very nearly so. Third, one sees no particular anomaly near the critical density, even at the lowest temperature. Fourth, one sees that the results depend only weakly on temperature.

Our results for the attractive mixture are shown in Figure 2. One sees that at the highest temperature the simulation and integral equation results agree well. However, at the intermediate

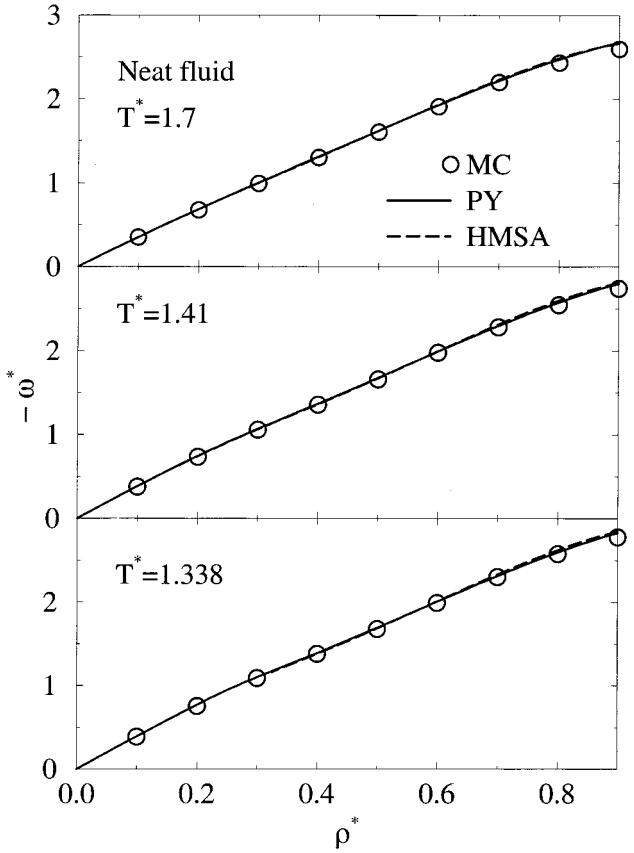

Figure 1. Vibrational frequency shifts versus density for the neat fluid at three different temperatures.

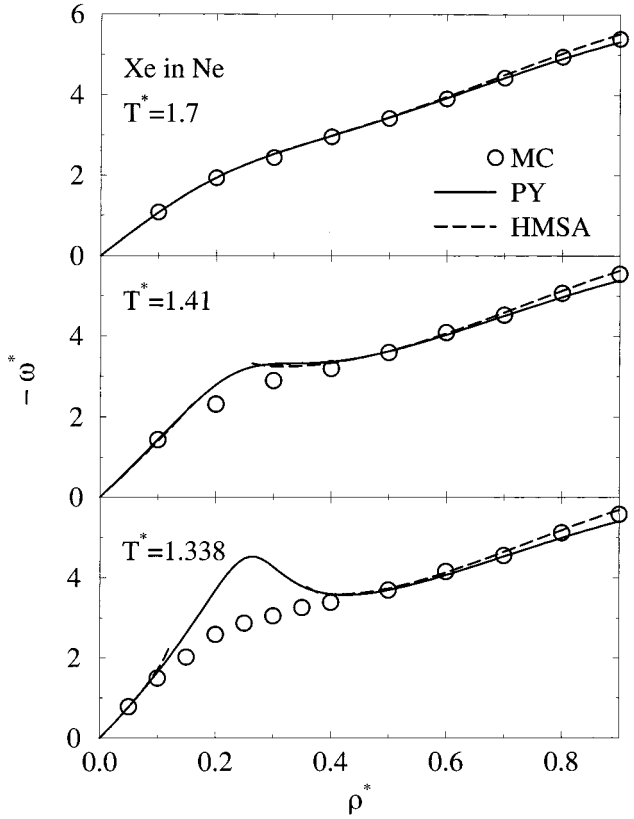

Figure 2. Vibrational frequency shifts versus density for the Xe in Ne attractive mixture at three different temperatures.

temperature there are clear discrepancies between the PY result and the simulation in the vicinity of the critical density. The same goes for the HMSA result, although here we could not obtain convergence in the near-critical region. At the lowest temperature we could not obtain converged HMSA results between $\rho^* = 0.12$ and 0.35, and the PY results are very inaccurate (compared to simulation) between $\rho^* = 0.1$ and 0.4. We have recently seen similar disagreements between PY and simulation results for $g(r)$ and for the solute's coordination number for an attractive mixture near the solvent's critical point.[43]

Regarding the density dependence in the case of the attractive mixture, one sees that from the simulation, especially at the lowest temperature, the frequency shift rises steeply as a function of density, then in the vicinity of the critical density the slope decreases markedly, and finally becomes somewhat steeper again at about $\rho^* = 0.5$. This peculiar nonlinear density dependence becomes less pronounced at higher temperatures.

This nonlinear density dependence follows very closely the density dependence of the solute's coordination number,[43] since, at least for this potential model, both the coordination number and the frequency shift are sensitive to the same feature of $g(r)$, namely the first peak. We interpreted[43] the density dependence of the coordination number as a crossover from an energy-dominated low-density slope, to a packing-dominated value at high density. At the lowest densities $g(r)$ is given simply by the Boltzmann factor $e^{-\phi(r)/kT}$, and the height of the first peak of $g(r)$ is $e^{\epsilon/kT} = e^{\epsilon/\epsilon_s T^*}$. Thus the value of the low-density slope depends sensitively on energetic factors (the potential well depths) and temperature, decreasing as the latter increases. In contrast, as is well known,[62] the coordination number at high densities is determined almost entirely from packing effects. For the attractive mixture the low-density slope extrapolates to a value higher than the high-density value. Furthermore, for the attractive mixture, which has a large solute−solvent well depth, the low density slope is indeed quite sensitive to temperature, decreasing with higher temperature, while the high-density packing value is nearly temperature independent. These observations therefore explain both the nonlinear density dependence of the frequency shift for attractive mixtures and the weakening of the effect as temperature is increased. In contrast, for the neat fluid, the low-density slope is less sensitive to temperature, and extrapolates nicely (by accident![43]) to the high-density value, and so the overall density dependence is nearly linear.

In summary, then, these model calculations do show the features seen experimentally: (1) for attractive mixtures the density dependence is nonlinear, changing slope near the critical density, (2) this nonlinearity becomes less pronounced for higher temperatures, (3) for neat fluids the density dependence is nearly linear, even for the near-critical isotherm. While our low-temperature result does not show a density plateau per se, it is possible that at lower temperatures (closer to T_c) and/or for more attractive mixtures, calculations would show something approaching a plateau.

One last comment before we conclude this section: The reason the frequency shift tracks the solute's coordination number for the model studied is that $f_1(r)$ is proportional to the reference LJ potential, which has its minimum near the peak of $g(r)$. Therefore, it is relatively slowly varying over the region where $g(r)$ is peaked, and so the integral up to a cutoff over $g(r)$ (the coordination number) is roughly proportional to the frequency shift. In contrast, if $\lambda_2 \neq 0$ but $\lambda_1 = 0$, and the primary dependence of the solute−solvent potential on q comes from the solute−solvent diameter, then the all-important factor of 2 in the definition of $f_2(r)$ changes things dramatically. Here, $f_2(r)$

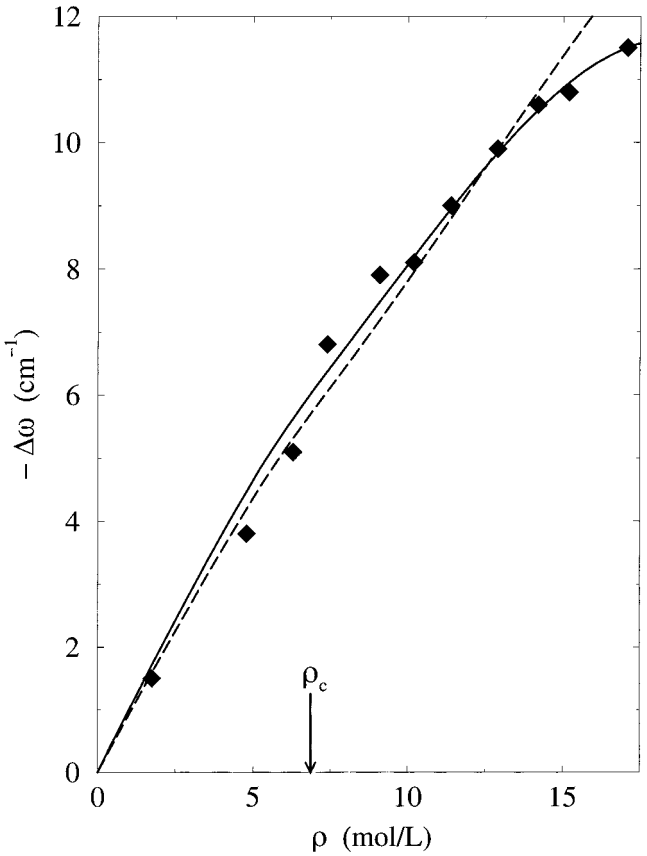

Figure 3. Vibrational frequency shift versus density for the symmetric CH stretch mode of neat ethane at 312 K. The diamonds are the experimental results, the dashed line is the one-parameter fit, and the solid line is the two-parameter fit.

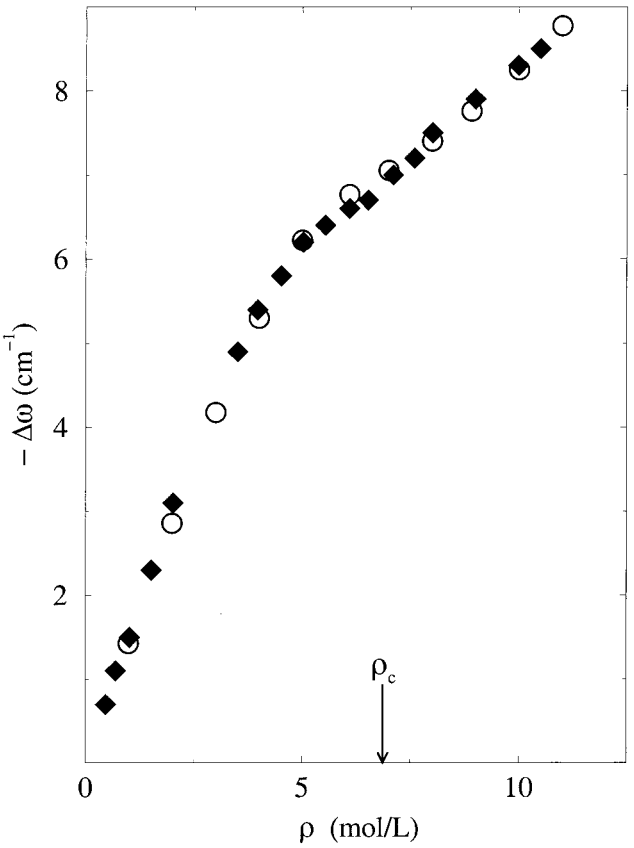

Figure 4. Vibrational frequency shift versus density for the asymmetric CO stretch mode of dilute $W(CO)_6$ in ethane at 307.15 K. The diamonds are the experimental results, and the circles are from theory.

is not slowly varying in the region of the maximum of $g(r)$, and so the frequency shift does not track the coordination number. In fact, for this model the frequency shift can start off negative at low density and become positive for higher densities. We have not shown calculations for this model since the resulting density dependence is quite different from that seen experimentally for near-critical temperatures. But in the next section we will consider the case where both λ_1 and λ_2 are nonzero.

V. Comparison between Theory and Experiment

The first set of experiments we examine are Raman line shifts of the CH symmetric stretch mode of neat supercritical ethane.[22] The experiments were performed as a function of density, from 3 to 17 mol/L, at $T = 312$ K. The critical temperature and density of ethane are $T_c = 305.33$ K and $\rho_c = 6.87$ mol/L. Therefore the experiments correspond to a reduced temperature of $T_r = 1.02$. The experimental data are shown in Figure 3.

In our model, ethane is to be represented by a Lennard-Jones sphere, whose parameters we choose so as to obtain the experimental critical constants. Using the simulation values for the LJ critical point mentioned earlier, this procedure yields $\sigma_s = 4.24$ Å and $\epsilon_s/k = 233$ K. For a neat fluid, $\sigma = \sigma_s$ and $\epsilon = \epsilon_s$. We calculate the frequency shift from eq 11, first assuming that $\lambda_2 = 0$, and perform a linear least-squares fit to the experimental data using λ_1 as the single adjustable parameter. In doing so we used the PY approximation to the Ornstein−Zernike equation, since from the model studies we know it to be accurate for the neat fluid at $T_r = 1.02$ and at densities in which we are interested. The results of this fit are also shown in Figure 3, and the agreement with experiment is good, at least up to a density of about 14 mol/L. The resulting value of λ_1 is 0.031ϵ. To describe better the curvature in the shift at high density, we can also consider a two-parameter fit, allowing both λ_1 and λ_2 to be nonzero. This result is also shown in Figure 3, and the fit is quite good. In this case the values of the parameters are $\lambda_1 = 0.030\epsilon$ and $\lambda_2 = 0.011\epsilon$.

The second set of data we consider involves the solute $W(CO)_6$ in supercritical ethane.[19] The data come from infrared line shape measurements of the asymmetric (T_{1u}) CO stretching mode as function of density from 0.5 to 10.5 mol/L at $T = 307.15$ K (which corresponds to $T_r = 1.006$). The experimental data are shown in Figure 4. Note that these data are not precisely those in ref 19. The authors of that work have recently realized that their published data in the close vicinity of the critical point are slightly in error due to a minor miscalibration of the pressure of the experimental cell and to small temperature variations within the apparatus. After these problems were eliminated the line shapes were remeasured,[63] and these new data appear in Figure 4. Also note that in plotting the frequency *shift* we have subtracted the isolated-solute frequency, 1997.0 cm^{-1}, from the measured line positions. This value was obtained by extrapolating the experimental results to the zero-density limit and is in fair agreement with the value of 1997.3 cm^{-1} measured recently.[63]

The application of our theory to this problem is more involved for two reasons. First, since it is not a neat fluid, there are in principle four (too many!) unknown parameters: ϵ, σ, λ_1, and λ_2. (σ_s and ϵ_s for ethane are taken from above.) To ameliorate this situation we obtain σ from a consideration of the crystal structure of $W(CO)_6$.[64] Modeling the solid state as a close-packed arrangement of spheres gives the effective diameter of

$W(CO)_6$ as 6.76 Å. Standard combining rules then produce a value for the solute−solvent diameter of $\sigma = 5.50$ Å, which is the value we use in the calculation. Since the vibrational mode in question is an asymmetric stretch, it seems likely that the effective size of the solute will not be strongly dependent on the vibrational coordinate, and so we set $\lambda_2 = 0$. This leaves two unknown parameters, ϵ and λ_1. The second complication is that from our model studies of the attractive mixture it is clear that the PY approximation is not at all reliable near the critical point (and the HMSA approximation does not converge), indicating that we cannot use this approximation in obtaining a global fit of the data. Moreover, performing a two-parameter global fit using Monte Carlo results is next to impossible, since for each value of ϵ simulations must be performed at many densities, each exploring millions of configurations, and then this must be repeated many times. To guide us in choosing a value for ϵ we performed HMSA calculations at low and at high densities, where we expect this approximation to be accurate. In addition, we performed a series of simulations for different ϵ values at one intermediate density. Comparing our line shift calculations from these results to experiment, we have chosen to take $\epsilon/k = 500$ K, which cannot be considered a true best-fit parameter, since we have not optimized it at several densities. Using this value of ϵ we then performed Monte Carlo simulations for a wide range of densities. Using these results we then adjusted λ_1 in order to get the best agreement with experiment, with the result $\lambda_1 = 0.0057\epsilon$. Using this value of λ_1 our simulation results are compared to experiment in Figure 4, and the agreement is excellent.

On one hand, one should not take the above comparisons with experiment too seriously. For example, we are the first to admit that neither ethane nor $W(CO)_6$ are spherical. In addition, our LJ models for the vibrational shifts are surely oversimplified. Nonetheless, the good fits to the data do suggest that our simple generic potential models can capture the essence of the observed phenomena.

VI. Conclusion

In this paper we have developed a theoretical treatment of solvent-induced spectral shifts in supercritical fluids based on a simple model of a dilute spherical solute in a fluid of spherical solvent particles. We have presented a microscopic expression for the vibrational solvatochromic shift, which involves interaction potentials and the solute−solvent radial distribution function. The latter was obtained from integral equations and Monte Carlo simulations.

We have performed model calculations of spectral shifts for a range of solvent densities and temperatures and model potential parameters. We were able to reproduce qualitatively the general trends observed experimentally: that for a neat fluid the frequency shift depends more or less linearly on density, while for an attractive solute−solvent mixture the frequency shift is nonlinear in density, the nonlinearity being more pronounced the more attractive the mixture and the closer to the critical temperature. The anomalous behavior of spectral shifts in the near-critical region was rationalized on the basis of the density dependence of the solute's coordination number, which in turn is due to a crossover from an energy-dominated to a packing-dominated regime.[43] We also performed quantitative comparisons of our theory with experimental data on vibrational spectral shifts for a neat fluid and for a mixture, and were able to reproduce experimental results quite well.

This work supports the picture that spectroscopic density anomalies are due to local density enhancement of the solvent in the vicinity of the solute.[4,13,27−36] As such, one can understand why SCFs can be such useful solvents: at near-critical densities (which are reduced significantly from those of a dense liquid), transport properties are superior to those of a liquid, while solvation properties can be nearly as good as those of liquids, since the coordination number of a solute in a near-critical fluid can be comparable to that in a dense liquid.[43]

Finally, we note that similar density anomalies have recently been observed for vibrational energy relaxation rates of polyatomic solutes in SCFs.[10,19] A fascinating temperature anomaly has also been observed: when the temperature of the SCF is increased (at constant density) the vibrational relaxation rate can decrease![19] As the theory of vibrational energy relaxation is somewhat more involved, it, as well as a comparison with experiment, will be published separately.[65] Here we simply note that, ultimately, we believe that the origin of the density anomaly in these experiments can also be traced back to the concept of local density enhancement in attractive mixtures.

Acknowledgment. J.L.S. thanks Michael Fayer for many helpful and spirited discussions. The authors are especially grateful to Dan Myers and Michael Fayer for providing their new line shift measurements prior to publication. The authors also thank Rich Stratt, Arun Yethiraj, Susan Tucker, Larry Dahl, Clark Landis, Steve Feldgus, and Biman Bagchi for helpful conversations, and Susan Tucker for sending a preprint of her review article. The authors appreciate the thorough and critical reading of the manuscript by one of the referees. The authors are grateful for support from the National Science Foundation (Grant Nos. CHE-9816235 and CHE-9522057).

References and Notes

(1) Kiran, E., Brennecke, J. F., Eds. *Supercritical Fluid Engineering Science*, ACS Symposium Series 514; American Chemical Society: Washington, D.C., 1993.
(2) Kiran, E., Singers, J. M. H. L., Eds. *Supercritical Fluids: Fundamentals for Applications*; Kluwer: Dordrecht, 1994.
(3) Eckert, C. A.; Knutson, B. L.; Debenedetti, P. G. *Nature* **1996**, *383*, 313.
(4) Tucker, S. C.; Maddox, M. W. *J. Phys. Chem. B* **1998**, *102*, 2437.
(5) Kauffman, J. *Anal. Chem.* **1996**, *68*, 248.
(6) Johnston, K. P.; Haynes, C. *AIChE J.* **1987**, *33*, 2017.
(7) Chester, T. L.; Pinkston, J. D.; Raynie, D. E. *Anal. Chem.* **1998**, *70*, 301R.
(8) Morita, A.; Kajimoto, O. *J. Phys. Chem.* **1990**, *94*, 6420−6425.
(9) Sun, Y.-P.; Bunker, C. E. *Ber. Bunsen-Ges. Phys. Chem.* **1995**, *99*, 976−984.
(10) Schwarzer, D.; Troe, J.; Zerezke, M. *J. Chem. Phys.* **1997**, *107*, 8380.
(11) Maiwald, M.; Schneider, G. M. *Ber. Bunsen-Ges. Phys. Chem.* **1998**, *102*, 960.
(12) Sun, Y.-P.; Bennett, G.; Johnston, K. P.; Fox, M. A. *J. Phys. Chem.* **1992**, *96*, 10001.
(13) Kajimoto, O.; Futakami, M.; Kobayashi, T.; Yamasaki, K. *J. Phys. Chem.* **1988**, *92*, 1347.
(14) Zhang, J.; Roek, D. P.; Chateauneuf, J. E.; Brennecke, J. F. *J. Am. Chem. Soc.* **1997**, *119*, 9980.
(15) Nowak, R.; Bernstein, E. R. *J. Chem. Phys.* **1987**, *86*, 3197.
(16) Nowak, R.; Bernstein, E. R. *J. Chem. Phys.* **1987**, *86*, 4783.
(17) Nowak, R.; Bernstein, E. R. *J. Chem. Phys.* **1987**, *87*, 2457.
(18) Otomo, J.; Koda, S. *Chem. Phys. Lett.* **1999**, *242*, 241.
(19) Urdahl, R. S.; Myers, D. J.; Rector, K. D.; Davis, P. H.; Cherayil, B. J.; Fayer, M. D. *J. Chem. Phys.* **1997**, 107, 3747.
(20) Akimoto, S.; Kajimoto, O. *Chem. Phys. Lett.* **1993**, *209*, 263.
(21) Echargui, M. A.; Marsault-Herail, F. *Mol. Phys.* **1987**, *60*, 605.
(22) Ben-Amotz, D.; LaPlant, F.; Shea, D.; Gardecki, J.; List, D. In *Supercritical Fluid Technology*, ACS Symposium Series 488; Bright, F. V., McNally, M. E., Eds.; American Chemical Society: Washington D.C., Amsterdam, 1992; p 144.
(23) Bizot, P.; Echargui, M. A.; Marsault, J. P.; Marsault-Herail, F. *Mol. Phys.* **1993**, *79*, 489.
(24) Pan, X.; McDonald, J. C.; MacPhail, R. A. *J. Chem. Phys.* **1999**, *110*, 1677.
(25) Clouter, M. J.; Kiefte, H.; Ali, N. *Phys. Rev. Lett.* **1978**, *40*, 1170.

(26) Wood, K. A.; Strauss, H. L. *J. Chem. Phys.* **1983**, *78*, 3455.
(27) Tucker, S. C. *Chem. Rev.* **1999**, *99*, 391.
(28) Kim, S.; Johnston, K. P. *AIChE J.* **1987**, *33*, 1603.
(29) Brennecke, J. F.; Tomasko, D. L.; Peshkin, J.; Eckert, C. A. *Ind. Eng. Chem. Res.* **1990**, *29*, 1682.
(30) Carlier, C.; Randolph, T. W. *AIChE J.* **1993**, *39* (5), 876.
(31) Zhang, J.; Lee, L. L.; Brennecke, J. F. *J. Phys. Chem.* **1995**, *99*, 9268.
(32) Schulte, R. D.; Kauffman, J. F. *Appl. Spectrosc.* **1995**, *49*, 31.
(33) Takahashi, K.; Abe, K.; Sawamura, S.; Jonah, C. D. *Chem. Phys. Lett.* **1998**, *282*, 361.
(34) Lu, J.; Han, B.; Yan, H. *Ber. Bunsen-Ges. Phys. Chem.* **1998**, *102*, 695.
(35) Flanagin, L. W.; Balbuena, P. B.; Johnston, K. P.; Rossky, P. J. *J. Phys. Chem.* **1995**, *99*, 5196.
(36) Kajimoto, O. *Chem. Rev.* **1999**, *99*, 355.
(37) Petsche, I. B.; Debenedetti, P. G. *J. Phys. Chem.* **1991**, *95*, 386.
(38) Wu, R.-S.; Lee, L. L.; Cochran, H. D. *J. Supercrit. Fluids* **1992**, *5*, 192.
(39) Wu, R.-S.; Lee, L. L.; Cochran, H. D. *Ind. Eng. Chem. Res.* **1990**, *29*, 977.
(40) Tom, J. W.; Debenedetti, P. G. *Ind. Eng. Chem. Res.* **1993**, *32*, 2118.
(41) Petsche, I. B.; Debenedetti, P. *G. J. Chem. Phys.* **1989**, *91*, 7075.
(42) Tanaka, H.; Shen, J. W.; Nakanishi, K.; Zeng, X. C. *Chem. Phys. Lett.* **1995**, *239*, 168.
(43) Egorov, S. A.; Skinner, J. L. *Chem. Phys. Lett.*, in press.
(44) Yonker, C. R.; Smith, R. D. *J. Phys. Chem.* **1988**, *92*, 235.
(45) Adams, J. *E. J. Phys. Chem. B* **1998**, *102*, 7455.
(46) Frankland, S. J. V.; Maroncelli, M. *J. Chem. Phys.* **1999**, *110*, 1687.
(47) Ben-Amotz, D.; Herschbach, D. R. *J. Phys. Chem.* **1993**, *97*, 2295.
(48) Schweizer; K. S.; Chandler, D. *J. Chem. Phys.* **1982**, *76*, 2296.
(49) Cherayil, B. J.; Fayer, M. D. *J. Chem. Phys.* **1997**, *107*, 7642.
(50) Saven, J. G.; Skinner, J. L. *J. Chem. Phys.* **1993**, *99*, 4391.
(51) Stephens, M. D.; Saven, J. G.; Skinner, J. L. *J. Chem. Phys.* **1997**, *106*, 2129.
(52) Egorov, S. A.; Stephens, M. D.; Skinner, J. L. *J. Chem. Phys.* **1997**, *107*, 10485.
(53) Parola, A.; Reatto, L. *Adv. Phys.* **1995**, *44*, 211.
(54) Herman, M. F.; Berne, B. J. *J. Chem. Phys.* **1983**, *78*, 4103.
(55) Egorov, S. A.; Skinner, J. L. *J. Chem. Phys.* **1996**, *105*, 7047.
(56) Zerah, G.; Hansen, J.-P. *J. Chem. Phys.* **1986**, *84*, 2336.
(57) Egorov, S. A.; Stephens, M. D.; Yethiraj, A.; Skinner, J. L. *Mol. Phys.* **1996**, *88*, 477.
(58) Hansen, J. P.; McDonald, I. R. *Theory of Simple Liquids*, 2nd ed.; Academic: London, 1986.
(59) Potoff, J. J.; Panagiotopoulos, A. Z. *J. Chem. Phys.* **1998**, *109*, 10914.
(60) Caillol, J. M. *J. Chem. Phys.* **1998**, *109*, 4885.
(61) Tang, Y. *J. Chem. Phys.* **1998**, *109*, 5935.
(62) Chandler, D.; Weeks, J. D.; Andersen, H. C. *Science* **1983**, *220*, 787.
(63) Myers, D. J.; Shigeiwa, M.; Fayer, M. D.; Cherayil, B. J. *J. Phys. Chem.*, submitted.
(64) Heinemann, F.; Schmidt, H.; Peters, K.; Thiery, D. *Z. Kristallogr.* **1992**, *198*, 123.
(65) Egorov, S. A.; Skinner, J. L. *J. Chem. Phys.*, in press.